Using otolith microchemistry to determine natal origin of Black Sea Bass off the coast of Maine

Elise R. Koob[a,*], Lisa A. Kerr[b], John W. Mandelman[c], Michael P. Armstrong[a]

[a] *Massachusetts Division of Marine Fisheries, Annisquam River Marine Station, 30 Emerson Avenue, Gloucester, MA 01930, USA*

[b] *University of Maine, Gulf of Maine Research Institute, 350 Commercial Street, Portland, ME 04101, USA*

[c] *Anderson Cabot Center for Ocean Life, New England Aquarium, 1 Central Wharf, Boston, Massachusetts 02110, USA*

*Corresponding author.

Email address: elise.koob@mass.gov (E.R. Koob)

[A]Abstract

A recent expansion of the northern stock of Black Sea Bass (*Centropristis striata*) into the northern Gulf of Maine raises questions about this species' movement and population dynamics in this region. Determining the origin of these fish is essential, as dramatic changes in migration patterns or current population boundaries could have profound effects on stock assessment estimates and subsequent management regulations. In this study, we measured otolith core concentrations of stable isotopes ($\delta^{18}O$, $\delta^{13}C$) and trace element:calcium ratios (Mg:Ca, Mn:Ca, Cu:Ca, Zn:Ca, Ba:Ca, Sr:Ca) to assess the natal origin of Black Sea Bass caught off the coast of Maine. Spawning condition adults from Southern New England (SNE) and the mid-Atlantic Bight (MAB) were used to characterize the chemical fingerprint of these known spawning regions. Unique chemical fingerprints were identified between SNE and MAB with high reclassification success using random forest analysis (16% error rate). Classification of Black Sea Bass of unknown origin caught in Maine waters indicated that 85% of the samples matched to SNE and 13% to the MAB, while one sample remained unclassified. Results from this study support the current management population separation of the northern stock of Black Sea Bass between SNE and MAB and lends additional information to the understanding of this species' movement into the northern Gulf of Maine. As fish stocks around the world continue to shift into new regions due to climate change, knowledge of their natal origin will be critical to long-term sustainable management of this species.

[A]Introduction

The northern stock of Black Sea Bass *Centropristis striata* is an important commercial and recreational finfish species extending from Cape Hatteras, North Carolina to the Gulf of Maine (Musick and Mercer 1977; Cadrin et al. 2016). In 2016, the northern stock was separated into two management subunits north and south of the Hudson Canyon (NEFSC 2017). Though this greater spatial detail allows for more nuanced stock assessment and management regulations, recent observations of Black Sea Bass as far north as Maine (SARC 2016; McMahan et al. 2020) raise additional concerns about the structure and movement patterns of this species. In recent years, commercial and recreational fishermen (Cadrin et al. 2016; McMahan 2017), as well as fishery-independent surveys (Miller et al. 2016), report an increasing abundance of Black Sea Bass in Maine, a region in which they were once rare (Collette and Klein-McPhee, 2002). These changes may be in response to the rapid warming of the Gulf of Maine (Pershing et al. 2015), either by migratory response (Nye et al. 2009) or an increase in reproductive productivity (McBride et al. 2018). As such, studies have shown that the northerly distribution trends of Black Sea Bass are associated with increasing temperatures of the northwest Atlantic (Bell et al. 2015; Kleisner et al. 2016; Miller et al. 2016).

This recent expansion into Maine waters is well documented, however, the natal origin of these fish is unknown. Black Sea Bass from Southern New England (SNE; north of the Hudson Canyon) migrate south and east in the fall to the outer continental shelf; whereas, fish from the mid-Atlantic Bight (MAB; south of the Hudson Canyon) migrate directly east (Mercer 1978; Able et al. 1995; Moser and Shepherd 2009). These populations return in the spring and exhibit spawning site fidelity (Kolek 1990; Able and Hales 1997; Fabrizio et al. 2013), though some straying to areas farther north has been observed (Moser and Shepherd 2009). The occasional

straying behavior of SNE fish is one theory as to how Black Sea Bass moved into the Gulf of Maine. It has also been suggested that fish or larvae are transported through the Cape Cod Canal from spawning activity in Buzzards Bay and advected north (G.R. Shepherd, National Marine Fisheries Service, personal communication; McBride et al. 2018). It is also important, however, to explore the possibility that fish spawned in the MAB have begun migrating north. Changes in migration or species distribution can have major implications on survivability, resource availability, and management (Fogarty et al. 2007; Kleisner et al. 2017), and no Gulf of Maine Black Sea Bass tagging studies have been published to address these concerns.

Otolith microchemistry is an established stock identification tool that can be used to identify fish that inhabit different environments and to infer stock structure (Elsdon et al. 2008; Kerr and Campana 2014). Otoliths are metabolically inert calcium carbonate structures that accrete layers daily, incorporating elements from the environment that are retained throughout a fish's life (Campana and Neilsson 1985; Campana 1999). Uptake and assimilation of elements into new otolith material can be influenced by environmental concentrations (Farrell and Campana 1996), water temperature or salinity (Fowler et al. 1995a; Hoff and Fuiman 1995; Thorrold et al. 1997a), growth rate (Sadovy and Severin 1992, 1994; Fowler et al. 1995a), physiological and metabolic regulation (Kalish 1989, 1991; Campana 1999), and diet (Farrell and Campana 1996). Consequently, fish encountering different environments will produce unique 'elemental fingerprints' (Campana et al. 2000; Campana and Thorrold 2001) that can be used to distinguish between populations, examine environmental history, categorize nursery grounds, track migration, and determine natal origins (Townsend et al. 1995; Thorrold et al. 1998; Campana et al. 2000; Gillanders 2002; Campana 2005; Tanner et al. 2012). Otolith fingerprint analysis has never been conducted on the northern stock of Black Sea Bass and

provides an opportunity to elucidate this species' movement into Maine waters. Determining whether fish caught in this area originate from a single stock unit, or a combination of SNE and MAB populations, is important for future management and conservation practices (Steer et al. 2009; Loewen et al. 2015; Tanner et al. 2016).

In microchemical studies, the natal origin of a group of fish is analyzed by targeting the otolith core, i.e., the time after hatch (Campana 1999, 2005; Arslan and Secor 2008), and matching the elemental fingerprint to those of potential spawning regions (Thresher 1999; Kerr et al. 2020). Black Sea Bass in the northern stock spawn along the Atlantic coast from Cape Hatteras through Massachusetts, but there is no evidence of active spawning north of Cape Cod, Massachusetts (McBride et al. 2018). Spawning populations of Black Sea Bass in SNE and MAB should have unique otolith core elemental fingerprints due to differences in behavior and migration, and thus should allow for natal origin identification of fish caught in Maine waters by matching these fingerprints (Campana et al. 1994, 2000).

Information gathered from otolith microchemistry can enhance our understanding of a species' population dynamics, which is imperative to the sustainable management of an exploited stock (Secor 1999; Artetxe-Arrate et al. 2019). The cause of Black Sea Bass movement north is poorly understood and shifts in distribution could impact thinking on the appropriate scale of management units and implementation of fishery regulations. The goals of this study were to (1) identify core elemental fingerprints of Black Sea Bass spawning regions (SNE and MAB), and; (2) use those fingerprints to classify the natal origin of fish caught in Maine waters.

[A]Methods

[C]*Sample selection.—*

Black Sea Bass exhibit a wide spatial range of spawning activity along the coast (from Cape Hatteras to Cape Cod), as opposed to congregating in discrete spawning locations (McBride 2017). Therefore, the population split at the Hudson Canyon (NEFSC 2017) was used to distinguish spawning regions rather than splitting the populations further into arbitrary segments. An archival collection of black sea bass otoliths was acquired from collaborators across the Northeast U.S. These otoliths were originally collected by collaborative institutions between May and November from 2013 to 2017 (Table 1). Samples were grouped into three regions based on capture location: ME (Maine), SNE (Massachusetts to the Hudson Canyon), and MAB (Hudson Canyon to Cape Hatteras; Figure 1).

Unfortunately, adequate young-of-the-year samples were not collected from the regions of interest in the years needed for this study. Due to Black Sea Bass' spawning site fidelity (Kolek 1990; Able and Hales 1997; Fabrizio et al. 2013) and stability of otolith core chemistry over time (Campana and Neilsson 1985), otolith cores from spawning condition fish were analyzed in this study to represent spawning regions (i.e., SNE and MAB). These samples were selected from fish with maturity codes of 'ripe' or 'ripe and running' at the time of capture. Fabrizio et al. (2014) observed that Black Sea Bass exhibit home ranges of 0.05 to 2.8 square miles in size between feeding and spawning grounds. The relative limited movement of spawning condition fish (compared to size of allocated regions) ensures that these samples represent Black Sea Bass spawning locations for this study (Campana 1999; Campana et al. 2000). The criteria used between collaborators for maturity staging was based off standards set by Burnett et al. (1989).

Black Sea Bass otoliths selected for analysis (between 40 and 50 from each region) were randomized across sex (Table 1, $n = 133$). Sample sizes were limited by fish that included

prerequisite maturity data (for SNE and MAB) and modest sampling currently occurring in ME. Left side otoliths were selected when feasible, though some right-side otoliths were used (n = 20). Variation in otolith microchemistry between regions was expected to be greater than any noise created from differences between left and right-side otoliths. Additionally, some studies have shown there were no significant differences between otoliths of the same fish (Thorrold et al. 1997b; Campana et al. 2000; Javor and Dorval 2014); therefore, the inclusion of both left and right-side otoliths in this study likely did not affect findings.

[C]*Otolith preparation.*—

The central opaque region of Black Sea Bass otoliths was targeted for analysis as it is noted to represent the first 1 to 4 months of life for this species (Wenner et al. 1986). Black Sea Bass in the northern stock spawn from April through October, peaking in June and July (Kolek 1990; Wuenschel et al. 2013; McBride et al. 2018). Age-0 juveniles display a high degree of site fidelity (Able and Hales 1997) and remain in natal regions from 1 to 6 months until fall migration (Fabrizio et al. 2013). Due to this variability, a fixed transect length was not used in this study as to avoid potentially incorporating material associated with time spent outside natal regions, which could dilute the core chemical signature. Therefore, the size of the opaque region of otoliths in this study was expected to vary slightly as an artifact of spawning date (Wenner et al. 1986; Laugier et al. 2015). Statistical analyses were conducted to ensure variation in core transect length did not contribute to variation in chemical concentrations (See *Statistical analysis*).

Otoliths were embedded using West System epoxy resin and hardener (Gougeon Brothers, Inc., Bay City, MI) in silicone molds and sectioned through the core (0.5 millimeters (mm) thick) using a low speed IsoMet diamond blade saw (Buehler, Lake Bluff, IL; Figure 2, A).

Sections were mounted to standard glass slides (eight samples per slide) using a small amount of Crystal Bond adhesive (Electron Microscopy Sciences, Hatfield, PA). Photographs of sections and measurements of otolith core transect lengths (opaque region only) were taken using a camera-microscope system (100x) and ImagePro Premier, vers. 9.1 (Media Cybernetics, Inc., Rockville, MD; Figure 2, B). Age determinations were made using a validated otolith ageing method (Koob et al. 2021) and two independent readers.

[C]*Microchemical analysis.*—

The use of archived otoliths precluded the possibility of matching water chemistry to otolith chemistry in this study, as none of the previous studies the black sea bass samples came from included water sampling protocols. Post hoc collection of water samples when this project originated and concluded (2017-2019) would have led to a time-period mismatch as compared to when the fish were in their first few months of life (i.e., otolith core analysis; year classes 2010-2015). Additionally, without intensive water chemistry sampling during the same period as the otolith material being analyzed had formed, it could be difficult to match water chemistry data with otolith microconstituents as there would only be a snapshot of water chemistry to compare to an integrated measure of otolith chemistry (e.g., across the first few months of life). For this study, we relied on previously established relationships between water chemistry and microchemical incorporation into otoliths when assessing how the variables we used vary with changing ocean conditions (e.g., Kalish 1989, 1991; Campana 1999; Elsdon and Gillanders 2002; Sturrock et al. 2015).

Laser ablation inductively coupled plasma mass spectrometry (LA-ICPMS) and gas bench isotope ratio mass spectrometry (GB-IRMS) were used in this study to measure trace elements and stable isotopes, respectively. These two methods allow for directed sampling of a

small region of interest (i.e., otolith core) versus analyzing whole otoliths, which would incorporate chemical information of the fish's entire life (Fowler et al. 1995a; Kerr et al. 2007).

[C]*Trace element analysis: LA-ICPMS.—*

Samples were analyzed using an ICPMS (NexION 2000C; PerkinElmer, Waltham, MA) with laser sampling (LSX-213 G2+ Nd:YAG; Teledyne CETAC Technologies, Omaha, NE) equipped with a HelEX II sample cell (Teledyne CETAC Technologies, Omaha, NE) at the Environmental Analytical Facility (EAF) at the University of Massachusetts Boston. Samples were viewed under reflected light, and transect lines were drawn across the opaque core of the otoliths for analysis (Figure 2, B). A pre-ablation transect was run before elemental assay to remove any surface contaminants (Campana et al. 1994; Thresher 1999). Otolith material along the drawn transect was vaporized by the laser and transported by argon gas to the ICPMS for isotopic composition analysis (Denoyer et al. 1991).

Laboratory recommendations for instrument specifications were used as follows: pre-ablation transect spot size of 50µm and a speed of 50 µm/s; sampling transect spot size of 30µm and a speed of 15µm/s; laser output at 20%. Three transects of MACS-3 pressed carbonate disc standard (US Geological Survey, Reston, VA) were run before and after each slide (eight samples). The isotopes analyzed were: Ca^{48}, Mg^{24}, Mg^{25}, Mg^{26}, Mn^{55}, Cu^{63}, Cu^{65}, Zn^{64}, Zn^{66}, Zn^{68}, Sr^{86}, Sr^{87}, Sr^{88}, Cd^{112}, Cd^{114}, Ba^{136}, Ba^{137} and Ba^{138}. Additionally, Si^{28} was monitored to confirm the laser was not ablating the glass slide below the sample section. Data reduction and processing were completed using Igor Pro 7 (WaveMetrics, Inc., Portland, OR) and Iolite (Iolite Software, University of Melbourne, AU) software to correct for instrument drift and standardize to MACS-3. Isotopic abundances were converted to parts per million (ppm), reported relative to Ca^{48}, and averaged across the entire transect. Cd^{112}, Cd^{114}, and Zn^{68} were removed from further

analysis due to a large proportion of erroneous values produced during LA-ICPMS analysis. Average limit of detection values (ppm) for each isotope were as follows: Mg^{24} = 0.041, Mg^{25} = 0.130, Mg^{26} = 0.770, Mn^{55} = 0.195, Cu^{63} = 0.274, Cu^{65} = 0.425, Zn^{64} = 0.326, Zn^{66} = 0.473, Sr^{86} = 1.543, Sr^{87} = 0.373, Sr^{88} = 0.089, Ba^{136} = 1.458, Ba^{137} = 0.057, Ba^{138} = 0.018. All isotope measurements were consistently above the corresponding limits of detection.

[C]*Stable isotope analysis: GB-IRMS.—*

Following LA-ICPMS analysis, otolith cores were milled using a New Wave Research MicroMill (Electro Scientific Industries, Portland, OR). Micromill specifications were set to laboratory recommendations, as follows: scan speed of 55 µm/s, 9 passes per sample, depth per pass at 55µm, and drill speed at 100%. The diameter of the carbide drill bit was 300µm. The entire opaque region of the otolith core was sampled for analysis (Figure 2, B). Milled sample material was collected onto weighing paper, folded, and placed in plastic vials. The micromill, drill bit, and sample slides were cleaned with pressurized air and 95% ethanol between each sample to prevent cross-contamination.

Milled otolith material was weighed using a microbalance and placed in clean glass instrument tubes at the EAF. Laboratory standards NBS-19, IA-R022, and $CaCO_3$ were weighed to match sample weights for each run (between 0.2 and 0.3mg) and placed in clean glass instrument tubes. Air was removed from sample and standards tubes by injecting helium gas, and the powdered material was reacted with 100µl of 100% phosphoric acid and allowed to digest at 25 ^{0}C for 24 hours. The resulting CO_2 gas in the sample tubes was analyzed for $\delta^{18}O$ and $\delta^{13}C$ using a gas chromatograph IRMS (Gas Bench II; Thermo Fisher Scientific, Inc., Waltham, MA) at the EAF. The $CaCO_3$ standard was run at the start of each analysis day, whereas NBS-19 and IA-R022 standards were run at the start, after every 9 to 12 samples, and at the end of each

analysis day. Isotope ratio measurements were calibrated based on repeated measurements of the standards and reported relative to the Vienna Pee Dee Belemnite standard for carbonate materials.

[C]*Statistical analysis.*—

By not using a fixed transect length for core analysis, the likelihood of variation in the amount of material analyzed between samples is increased. Otolith core transect measurements were compared between regions using one-way analysis of variance (ANOVA) followed by Tukey's Honestly Significant Differences (Tukey's HSD). Additionally, in cases with significant ANOVA results, Pearson's correlation coefficients were used to examine correlations between mean core measurements and isotope ratios in each region (Thorrold et al. 1998). Scatter plots of each isotopic and elemental ratio by core measurement for each region were also assessed visually to determine the presence of any patterns relating to quantity of core material analyzed and measured concentrations.

Pearson's correlation coefficients between isotopes of the same element were also used to identify correlations between elements (Campana et al. 1994). All within-element correlations were high ($0.81 \leq r \leq 0.99$); therefore, the following isotopes were used in subsequent analyses to avoid redundancy: Mg^{24}, Mn^{55}, Cu^{63}, Zn^{64}, Sr^{86}, Ba^{137}, in addition to $\delta^{18}O$ and $\delta^{13}C$. All trace elements were expressed as element:Ca ratios. Data transformations were necessary for element:Ca distributions to satisfy normality assumptions. Mg:Ca, Mn:Ca, and Ba:Ca were $\log_{10}$ transformed ($\log_{10}(1+X)$); while Cu:Ca and Zn:Ca required inverse transformations ($1/(X+1)$). Sr:Ca, $\delta^{18}O$, and $\delta^{13}C$ were not transformed. Normality and homogeneity of variance and covariance were assessed using diagnostic plots, the Shapiro-Wilk test, and Levene's test. All elements passed Levene's test for homogeneity ($P > 0.05$). Shapiro-Wilk's test for normality was

passed by all elements ($P > 0.05$) except $\delta^{13}C$ ($P = 0.0051$). Inspection of $\delta^{13}C$ diagnostic plots showed a very slight left-skewed distribution, not a large departure from normality; therefore, parametric tests were considered suitable for this isotope. One outlier from Mg:Ca, with a value approximately 5 standard deviations above mean, was removed from analyses (Campana 2005).

Multivariate analysis of variance (MANOVA) using *Region* and *Year Class* (for regional interannual variation) as predictor variables and eight isotopes (Mg:Ca, Mn:Ca, Cu:Ca, Zn:Ca, Sr:Ca, Ba:Ca, $\delta^{18}O$ and $\delta^{13}C$) as response variables was used to identify differences in core chemical fingerprints. The MANOVA was used with Pillai's trace, which is robust to deviations in normality (Ateş et al. 2019). Individual ANOVAs and Tukey's HSD were conducted for isotopes with significant interactions. Isotopic and elemental ratio differences between regions were modeled with separate linear mixed models and tested for significance using Wald X^2-tests and post-hoc multiple comparison analyses with Tukey's HSD. In all models, *Region* was included as a fixed effect and *Year Class* as a random effect. Plots by region for each isotopic and elemental ratio were produced using back-transformed estimated marginal means (Lenth 2019) to help visualize differences.

Classification of ME samples to spawning regions was completed using random forest analysis (RF; Breiman 2001). This analysis used composite otolith signatures due to insufficient sample sizes in several of the year classes. A RF model including all isotopic and elemental ratios as predictors was assessed for variable importance by analyzing mean decrease in Gini coefficient (Breiman 2001). From these results, a base model built using $\delta^{18}O$, Mg:Ca, Cu:Ca, Mn:Ca, and Ba:Ca as predictors was compared to models with stepwise addition and subtraction of the remaining variables ($\delta^{13}C$, Zn:Ca, and Sr:Ca). The model with the lowest average 'out-of-bag' (OOB) error rate was selected as the discrimination function to classify samples

with unknown group membership (i.e., ME) to the spawning population with the highest probability of origin (i.e., SNE or MAB; Manel et al. 2005). The model's built-in cross validation procedure using bootstrap aggregation (Breiman 2001) was used instead of formal training and testing sets due to low sample sizes in this study. To avoid losing data, the probability threshold used was 0.50. Functions to optimize RF parameters of *ntree* and *mtry* indicated the default values (500 and 2, respectively) produced the lowest error, as illustrated in other studies (Liaw and Wiener 2002; Díaz-Uriarte and Alvarez de Andrés 2006).

All statistical tests in this study used a significance level of 0.05 and type III sums of squares were used where appropriate due to slightly unbalanced data. Visual assessment of diagnostic plots found that all models used in this study conformed to test assumptions. Analyses and visualizations were conducted using base R (version 3.6.1; R Core Team (2019), as well as the following packages: 'car' version 3.0-3 (Fox and Weisberg 2019), 'DHARMa' version 0.4.4 (Hartig 2021), 'emmeans' version 1.4.1 (Lenth 2019), 'ggord' version 1.1.6 (Beck 2021), 'ggplot2' version 3.2.1 (Wickham 2016), 'glmmTMB' version 1.0.2.1 (Brooks et al. 2017), 'multcomp' version 1.4-10 (Hothorn et al. 2008), 'MASS' version 7.3-51.1 (Venables and Ripley 2002), and 'randomForest' version 4.6-14 (Liaw and Wiener 2002).

[A]Results

[B]Otolith core measurements

Measurements of otolith cores ranged from 0.48 mm to 1.02 mm, which was slightly smaller than measurements taken by Wenner et al. (1986) for Black Sea Bass in the southern Atlantic stock (0.56 mm to 1.54 mm). Core measurements differed across regions ($F = 4.09$; df = 2; $P = 0.019$) and post-hoc analysis indicated ME core measurements were similar to MAB ($P > 0.05$), but statistically smaller than SNE ($P < 0.05$). Mean Pearson's correlation coefficients

between core measurements and isotopic and elemental ratios for each region were low, ranging between -0.33 to 0.36 and 16 out of 24 coefficients were negative (Figure 3). Therefore, in most regions, an increase in core transect length did not correspond to an increase in the isotopic and elemental ratios. Additionally, inspection of individual isotopic and elemental ratio plots by core measurement for each region indicated no clear visual patterns between isotopic and elemental ratios and core measurements. These results signify there was little concern of systematic effects on chemical concentrations attributable to core transect length in this study. Furthermore, mean core measurements for ME, SNE, and MAB were 0.70 mm, 0.77 mm, and 0.76 mm, respectively, demonstrating only a 0.01 mm difference between SNE and MAB and the resulting statistical difference.

[B]Regional otolith microchemical differences

The MANOVA detected an interaction between *Region* and *Year Class* (Pillai's Trace = 0.83; $F = 1.48$; df = 9; $P = 0.007$) for $\delta^{13}C$ ($F = 2.35$; df = 9; $P = 0.018$) and Mn:Ca ($F = 3.01$; df = 9; $P = 0.003$). Measurements of core $\delta^{13}C$ in ME in 2010, 2011, and 2012 were larger than in 2014 ($P < 0.05$); and 2013 was similar to all other year classes. Year classes within SNE and MAB were not significantly different for $\delta^{13}C$. Measurements of core Mn:Ca in ME were higher in 2010 than 2011 ($P < 0.05$), but both years were similar to 2012-2014. Mn:Ca varied by year class in SNE, where 2010 was lower than 2013 and 2014 ($P < 0.05$), but those year classes were similar to 2011, 2012, and 2015 ($P > 0.05$). See Appendix, Figure A.1, for visual depiction of isotopic and elemental ratios by year class for each region. Note this figure highlights the differences in sample sizes for some Year Class and Region combinations, which could contribute to the perceived interannual variability depicted in the analysis discussed here.

Results from the linear mixed model analysis showed that levels of $\delta^{18}O$, Mg:Ca, Mn:Ca, Cu:Ca, and Ba:Ca differed significantly across regions ($P < 0.05$); whereas Sr:Ca and $\delta^{13}C$ did not ($P > 0.05$; Figure 4). Wald X^2 result for Zn:Ca was significant ($P = 0.03$), but post-hoc analysis indicated no significant differences between region pairs ($P > 0.05$). Post-hoc analyses revealed that ME and SNE have lower $\delta^{18}O$, but higher Mg:Ca and Ba:Ca values than the MAB ($P < 0.05$). Mn:Ca in ME was lower than MAB ($P < 0.05$), but SNE was not different from either region ($P > 0.05$). Cu:Ca was lower in ME than both SNE and MAB ($P < 0.05$), which were similar to each other ($P > 0.05$). Untransformed mean signatures for each region, Wald X^2, and P values for each elemental ratio are shown in Table 2.

[B]*Discrimination and classification*

Variable importance for the RF model between SNE and MAB using all isotopic and elemental ratios indicated the most influential variable for classification was Ba:Ca, followed by $\delta^{18}O$, Mg:Ca, Cu:Ca, Mn:Ca, Zn:Ca, $\delta^{13}C$, and Sr:Ca. A model including all isotopic and elemental ratios resulted in the lowest OOB error rate (16%) and classified 39 of ME samples (85%) to SNE and 6 (13%) to the MAB. One sample was unassigned (assignment probability of 0.50 to each region). For samples assigned to SNE, there was a maximum assignment probability of 0.96 and an overall average probability of 0.82. The maximum probability of samples assigned to MAB was 0.76, with an overall average probability of 0.67.

[A]Discussion

[B]Regional discrimination and core chemical differences

This study showed that elements incorporated into Black Sea Bass otoliths during the first few months of life could be used to discriminate between spawning groups of fish. Otolith $\delta^{18}O$, Ba:Ca, and Mg:Ca were the most informative for discrimination between SNE and MAB

spawning groups. The remaining isotope and elemental ratios helped reduce error in the RF model and contributed to the discrimination between these regions. Each of these elements and isotopes are indicators of different processes and their abundance in the environment can be influenced by many factors. Additionally, incorporation of chemical signatures into otolith material is shown to vary with exogenous and endogenous processes, many times interactively, and can differ between element, location, and fish species (Kalish 1989; Fowler et al. 1995b, 1995a; Thorrold et al. 1997b; Hamer and Jenkins 2007; Barnes and Gillanders 2013; Sturrock et al. 2015). While such variability is difficult to decipher in this study, especially when controlled experimentation was not possible, we discuss several potential explanations driving the primary observed differences between regions.

Temperature has a well-documented, negative relationship with $\delta^{18}O$ in otoliths (Kalish 1991; Thorrold et al. 1997a; Elsdon and Gillanders 2002; Dorval et al. 2011; Carvalho et al. 2017). Thus, lower $\delta^{18}O$ levels in otoliths from MAB were expected compared to SNE, due to generally higher water temperatures in that region; however, the opposite was observed. These results could be explained by the differences in depth in Black Sea Bass spawning regions in this study. Many of the spawning adults collected from SNE were from Buzzards Bay and Nantucket Sound, where depths range from approximately 20 feet to 60 feet, versus depths from approximately 50 to 80 feet (though some up to 150 feet) for samples collected in the MAB (Office of Coast Survey 2022). Differences in bottom temperatures for these regions in 2016 and 2017 are highlighted in Figure A.2 where, for several months of the spawning season, Buzzards Bay (and at times the deeper Rhode Island Sound region) are warmer than the spawning areas off the New Jersey coast. Previous Black Sea Bass studies have reported high temperatures in Buzzards Bay and Nantucket Sound during the spawning season (+20^{0}C; Caruso 1995; McBride

et al. 2018) as well as relatively cool temperatures (13^0C) off the coast of New Jersey in the summer (Fabrizio et al. 2014). Further, other studies have also noted warmer temperatures at Black Sea Bas sampling sites in Massachusetts waters as compared to sampling areas in the MAB (Able et al. 1995; Slesinger et al. 2021). Differences in the depths of spawning habitats in these regions and subsequent variation of temperature dynamics likely explain the δ^{18}O results observed in this study between SNE and MAB.

Elsdon and Gillanders (2002) showed that Ba:Ca otolith concentrations increased with increased water temperatures. This supports the observation of higher concentrations of Ba:Ca in SNE as compared to MAB in this study, in accordance with the previously discussed temperature differences between sampling locations. A similar pattern of a higher Mg:Ca ratio in SNE than in MAB was observed; however, temperature's influence on the incorporation of this elemental ratio into otolith material is less distinct (Hoff and Fuiman 1995; Bath et al. 2000; Elsdon and Gillanders 2002). Studies have shown a substantial influence of physiological regulation on Mg:Ca incorporation into otoliths (Hamer and Jenkins 2007; Barnes and Gillanders 2013), making it difficult to infer the specific mechanisms causing the regional variability in this study. Despite these unknowns, the similarity in δ^{18}O, Ba:Ca, and Mg:Ca measurements between the SNE and ME samples suggest that Black Sea Bass from these regions came from similar natal regions.

Patterns between concentrations of Mn:Ca and Cu:Ca between regions in this study are more difficult to explain. Measurements of both these elemental ratios are similar between SNE and MAB. The main sources for manganese and copper in marine environments are river outflow, anthropogenic runoff, and sediment disturbance (Kremling 1985; Shiller 1997; VanHulten et al. 2017). Based on MAB sampling locations (Figure 1), higher Mn:Ca and Cu:Ca

measurements could be anticipated in this group due to the proximity of the Hudson River outflow. However, the expected transport of the Hudson River outflow along the New Jersey coast does not occur during the summer months (i.e., the Black Sea Bass spawning period) and instead, a freshwater bulge is created and forced north along the Long Island coast (Chant 2008). This may reduce the likelihood that Black Sea Bass larvae off the coast of New Jersey in the summer experience an extreme influx of these elements and instead this region may have similar concentration profiles to those in SNE, as seen in the otolith core concentrations in this study. The reason for the lower level of Cu:Ca in ME Black Sea Bass is unclear; further work is needed to examine the basis and implications of this finding.

Comparable δ^{13}C and Zn:Ca values between regions were expected because otolith concentrations of these elemental ratios are influenced by diet (Kalish 1991; Thorrold et al. 1997a; Ranaldi and Gagnon 2008). Though there may be some variation in specific prey consumed, Black Sea Bass are feeding at the same trophic level between regions (McMahan et al. 2020). Measured otolith Sr:Ca was also not expected to differ between regions in this study because the concentration of strontium in the marine environment remains relatively constant (Thorrold et al. 1997b; Elsdon et al. 2008).

[B]Natal origin, importance to management, and recommendations

Despite the limitations in understanding the regional variation of elements and their incorporation into otolith core structure in this study, the isotopic and elemental ratios used here are shown to be suitable geographic indicators to infer population structure and identify natal origin (Campana et al. 1994, 2000; Elsdon et al. 2008; Steer et al. 2009; Hüssy et al. 2020). Black Sea Bass spawning regions in this study, SNE and MAB, were shown to have different otolith core chemical fingerprints. This not only supports the population separation of the

northern stock between SNE and MAB imposed in the most recent stock assessment, but also allowed for the classification of Black Sea Bass caught in ME to a specific spawning region.

Most of the ME samples (85%) were classified to SNE, with a high average assignment probability. Fish caught in ME likely were either transferred through the Cape Cod Canal or gradually 'strayed' from their SNE spawning regions into waters farther north. Thus far, little work has been completed looking at Black Sea Bass transference through the Cape Cod Canal, either through adult migration or advection of larvae or juveniles. Moser and Shepherd (2009) observed a high rate of return to spawning locations for tagged Black Sea Bass (>90%) but also noted some straying behavior. Strays (defined as capture 1-degree of latitude and longitude from the release location) were more prevalent in fish tagged north of the Hudson Canyon than south: 6% versus 0.005%, respectively. Therefore, it is possible Black Sea Bass from SNE strayed into the southern Gulf of Maine when returning from seasonal migrations and have since started straying farther north into Maine waters.

Overall, the results presented herein do not support a dramatic change in the migration patterns of the MAB population. It is possible the six fish from ME assigned to MAB (as well as the one unclassified sample) could be examples of very rare straying events from that region. However, Moser and Shepherd (2009) observed an extremely low rate of fish tagged south of the Hudson Canyon and recovered in north (0.7%), indicating that this type of movement has not been common in the past for this species. There was less certainty in the assignment of ME samples to the MAB as compared to those assigned to SNE (average assignment probabilities of 0.67 and 0.82, respectively). This could signify that the samples assigned to MAB originated closer to Long Island Sound, near the Hudson Canyon population split. Otolith core chemistry from fish in this region may reflect a gradation in chemistry between SNE and MAB values,

leading to more ambiguity in chemical signatures and less certainty in assignment. The otolith archive used to draw samples from for this study did not contain Black Sea Bass otoliths with the necessary associated biological information (e.g., spawning condition) from Long Island Sound and could not be represented in this study. Additional work is needed on Black Sea Bass from this area to address fish that spawn near the stock boundaries.

Little is known about this species' movement, interactions, or potential for long-term success in Maine waters. A basic understanding of these fish's life history characteristics can be garnered from the population they originated from. The information from this study suggests that Black Sea Bass caught in Maine should have life history characteristics more similarly related to Black Sea Bass in SNE, rather than MAB. This is beneficial information to future stock assessments looking to incorporate data from catches farther north. However, it should be noted that recent work by McMahan et al. (2020) suggests that Black Sea Bass in Maine waters grow faster and reach maturity at a younger age than those caught in northern and southern Massachusetts (i.e., SNE). These findings highlight the need for additional research on Black Sea Bass life history, movement, behavior, and possible residency in Maine waters. This was the first otolith chemical fingerprinting study completed for this species, thus, there is a wide range of opportunities to use this technique to learn more about Black Sea Bass stock structure and migration patterns.

[B]Assumptions and other considerations

[C]*Interannual variation.—*

Use of archived otoliths and associated data limitations in this study (e.g., availability of maturity data) led to the use of multiple year classes. The multivariate analysis including an interaction between region and year class was conducted to identify interannual variability within

each region. Significant variability was seen only in ME for $\delta^{13}C$ and Mn:Ca for ME and SNE. Year Class was included as a random effect in the linear mixed models because, although other region and isotopic or elemental ratio combinations did not result in statistically significant findings, some variation was clear (and expected) among all groups (Figure A.1). Year Class could not be included in the RF model due to low sample size, however, the low OOB error rate for the SNE and MAB classification function suggests the analysis of multiple year classes and identification of multi-year regional chemical fingerprints in this study was successful and may give the opportunity for further use in the future (Brown 2006; Tournois et al. 2013). The authors identify that this study was exploratory in nature as well as its limitations regarding sample sizes and assessing interannual variability. Future studies should focus on fewer year classes and that the stability of microchemical signals over time should be tested with additional sampling.

[C]*No spawning in ME.—*

This study operates under the assumption that no Black Sea Bass spawning was occurring in Maine waters prior to 2016, which appears to be sound given the current information available. McBride et al.'s (2018) analysis of bottom-trawl survey data indicated that few spawning condition (or spent) females were found in the upper Gulf of Maine, which "would provide the most direct evidence of spawning." Additionally, the Northeast Fisheries Science Center survey extends to mid-coast Maine (~44^{0}N), but the northernmost occurrence of Black Sea Bass young-of-the-year or developing females were 42^{0}N (just north of Boston; McBride et al., 2018). Additionally, McMahan (2017) only observed young-of-the-year in Massachusetts waters (mostly south of Cape Cod), none farther north. Thus, based on the information available, it is unlikely that Black Sea Bass spawning occurred in Maine waters during the years used in this study.

[C]*Maternal transfer.*—

Previous studies have shown elevated concentrations of certain elements in the otolith primordium (Laugier et al. 2015; Artetxe-Arrate et al. 2019; Maguffee et al. 2019), often attributed to maternal transfer during egg development (Ruttenberg et al. 2005). There is concern that primordia concentrations do not accurately reflect the natal region and instead represent the water chemistry surrounding the female during gonadal development (Ben-Tzvi et al. 2007; Artetxe-Arrate et al. 2019). Black Sea Bass begin inshore migration to spawning locations from offshore overwintering grounds by April (Drohan et al. 2007) and the start of stage 3 of oogenesis, representing the start of ovarian activity, begins in May for this species (Mercer 1978). This data suggests ovary development does not occur until after the spring migration inshore has begun; therefore, any elemental incorporation from the environment by the female and transferred to the eggs should have occurred within the spawning regions identified in this study.

[A]Conclusions

Unique core elemental fingerprints for Black Sea Bass spawning regions (SNE and MAB) were identified in this study and used to classify Black Sea Bass caught in Maine waters, a region in which this species has not historically been known to inhabit in large numbers. Sample assignments were largely of SNE origin, though several individuals were assigned to MAB. Based on these results, a substantial number of Black Sea Bass spawned in the MAB traveling to ME is unlikely; however, additional research is needed to fully understand this species' movement into this new region. Future stock assessments looking to include catch data from northern regions could use these findings as a foundation that Black Sea Bass in Maine waters should have life history characteristics more closely associated to Black Sea Bass in SNE.

Additionally, the identification of defined otolith chemical fingerprints and successful discrimination of known samples between SNE and MAB support the 2016 management population separation of the northern stock of Black Sea Bass. The results of this work begin to provide insight on the possible population composition of Black Sea Bass in Maine waters, though recent trends of continuing propagation of this species into this region highlights the need for research on residency and their potential for future spawning activity.

[A]Acknowledgements

We thank NEFSC (E. Robillard; S. Sutherland; G. Shepherd; R. McBride), Rutgers Univ. (D. Zemeckis; M. Burglund), Northeastern Univ. (M. McMahan), RI-DEM (N. Lengyel), CFRF (T. Heimann), and VIMS (J. Garland) for samples and contacts, and Z. T. Whitener, A. Johnston, and A. Stebbins for training on sample processing. This work was supported by the National Marine Fisheries Service (award no. NA17NMF4740143), in cooperation with the Atlantic Coastal Cooperative Statistics Program, and from the U.S. Fish and Wildlife Service's Sport Fish Restoration Program (award no. F17AF00216 and no. F18AF00918).

[A]References

Able, K. W., M. P. Fahay, and G. R. Shepherd. 1995. Early life history of black sea bass, Centropristis striata, in the mid-Atlantic Bight and a New Jersey estuary. Fishery Bulletin 93:429–445.

Able, K. W., and L. S. Hales. 1997. Movements of juvenile black sea bass Centropristis striata (Linnaeus) in a southern New Jersey estuary. Journal of Experimental Marine Biology and Ecology 213:153–167.

Arslan, Z., and D. H. Secor. 2008. High resolution micromill sampling for analysis of fish otoliths by ICP-MS: Effects of sampling and specimen preparation on trace element fingerprints. Marine Environmental Research 66:364–371.

Artetxe-Arrate, I., I. Fraile, D. A. Crook, I. Zudaire, H. Arrizabalaga, A. Greig, and H. Murua. 2019. Otolith microchemistry: a useful tool for investigating stock structure of yellowfin tuna (Thunnus albacares) in the Indian Ocean. Marine and Freshwater Research 70:1708–1721.

Ateş, C., Ö. Kaymaz, H. E. Kale, and M. A. Tekindal. 2019. Comparison of test statistics of nonnormal and unbalanced samples for multivariate analysis of variance in terms of type-I error rates. Computational and Mathematical Methods in Medicine:1–8.

Barnes, T. C., and B. M. Gillanders. 2013. Combined effects of extrinsic and intrinsic factors on otolith chemistry: implications for environmental reconstructions. Canadian Journal of Fisheries and Aquatic Sciences 70:1159–1166.

Bath, G. E., S. R. Thorrold, C. M. Jones, S. E. Campana, J. W. McLaren, and J. W. H. Lam. 2000. Strontium and barium uptake in aragonitic otoliths of marine fish. Geochimica et Cosmochimica Acta 64(10):1705–1714.

Beck, M. W. 2021. Ggord: Ordination Plots with ggplot2. R Package version 1.1.6.

Bell, R. J., D. E. Richardson, J. A. Hare, P. D. Lynch, and P. S. Fratantoni. 2015. Disentangling the effects of climate, abundance, and size on the distribution of marine fish: an example based on four stocks from the Northeast US shelf. ICES Journal of Marine Science 72(5):1311–1322.

Ben-Tzvi, O., A. Abelson, S. D. Gaines, M. S. Sheehy, G. L. Paradis, and M. Kiflawi. 2007. The inclusion of sub-detection limit LA-ICPMS data, in the analysis of otolith microchemistry, by use of a palindrome sequence analysis (PaSA). Limnology and Oceanography: Methods 5:97–105.

Breiman, L. 2001. Random forests. Machine Learning 45:5–32.

Brooks, M. E., K. Kristensen, K. J. van Benthem, A. Magnusson, C. W. Berg, A. Nielsen, H. J. Skaug, M. Maechler, and B. M. Bolker. 2017. glmmTMB balances speed and flexibility among packages for zero-inflated generalized linear mixed modeling. The R Journal 9(2):378–400.

Brown, J. A. 2006. Classification of juvenile flatfishes to estuarine and coastal habitats based on the elemental composition of otoliths. Estuarine, Coastal and Shelf Science 66:594–611.

Burnett, J., L. O'Brien, R. K. Mayo, J. A. Darde, and M. Bohan. 1989. Finfish maturity sampling and classification schemes used during Northeast Fisheries Center bottom trawl surveys, 1963-89. NOAA Technical Memorandum NMFS-F/NEC:1–14.

Cadrin, S., R. Leaf, and O. Jensen. 2016. Contributions to the SAW62 black sea bass stock assessment. Science Center for Marine Fisheries:1–6.

Campana, S. E. 1999. Chemistry and composition of fish otoliths: pathways, mechanisms and applications. Marine Ecology Progress Series 188:263–297.

Campana, S. E. 2005. Otolith elemental composition as a natural marker of fish stocks. Pages 227–245 *in* S. X. Cadrin, K. D. Friedland, and J. R. Waldman, editors. Stock Identification Methods: Applications in Fishery Science. Academic Press, New York, USA.

Campana, S. E., G. A. Chouinard, J. M. Hanson, A. Frechet, and J. Brattey. 2000. Otolith elemental fingerprints as biological tracers of fish stocks. Fisheries Research 46:343–357.

Campana, S. E., A. J. Fowler, and C. M. Jones. 1994. Otolith elemental fingerprinting for stock identification of Atlantic Cod (Gadus morhua) using laser ablation ICPMS. Canadian Journal of Fisheries & Aquatic Sciences 51:1942–1950.

Campana, S. E., and D. Neilsson. 1985. Microstructure of fish otoliths. Canadian Journal of Fisheries & Aquatic Sciences 42:1014–1032.

Campana, S. E., and S. R. Thorrold. 2001. Otoliths, increments, and elements: keys to a comprehensive understanding of fish populations? Canadian Journal of Fisheries & Aquatic Sciences 58(1):30–38.

Caruso, P. G. 1995. The biology and fisheries of black sea bass (Centropristis striata) in Massachusetts waters. Univ. Rhode Island, Kingston, RI.

Carvalho, M. G., C. Moreira, J. F. M. F. Cardoso, G. J. A. Brummer, P. van Gaever, H. W. van der Veer, H. Queiroga, P. T. Santos, and A. T. Correia. 2017. Movement, connectivity and population structure of the intertidal fish Lipophrys pholis as revealed by otolith oxygen and carbon stable isotopes. Marine Biology Research 13(7):764–773.

Chant, R. J., J. Wilkin, W. Zhang, B.-J. Choi, E. Hunter, R. Castelao, S. Glenn, J. Jurisa, O. Schofield, R. Houghton, J. Kohut, T. K. Frazer, and M. A. Moline. 2008. Dispersal of the Hudson River plume in the New York Bight. Ocenography 21(4):148–161.

Collette, B.B., and Klein-McPhee, eds. 2002. Bigelow and Schroeder's Fishes of the Gulf of

Maine. Smithsonian Institution Press, Washington, DC, 748pp.

Denoyer, E. R., K. J. Fredeen, and J. W. Hager. 1991. Laser solid sampling for inductively coupled plasma mass spectrometry. Analytical Chemistry 63(8):445–457.

Díaz-Uriarte, R., and S. Alvarez de Andrés. 2006. Gene selection and classification of microarray data using random forest. BMC Bioinformatics 7(3):1–13.

Dorval, E., K. Piner, L. Robertson, C. S. Reiss, B. Javor, and R. Vetter. 2011. Temperature record in the oxygen stable isotopes of Pacific sardine otoliths: experimental vs. wild stocks from the Southern California Bight. Journal of Experimental Marine Biology and Ecology 397:136–143.

Drohan, A. F., J. P. Manderson, and D. B. Packer. 2007. Essential fish habitat source document: black sea bass, Centropristis striata, life history and habitat characteristics. Pages 227–245, NOAA Technical Memorandum NMFS-NE-200. Woods Hole, MA.

Elsdon, T. S., and B. M. Gillanders. 2002. Interactive effects of temperature and salinity on otolith chemistry: challenges for determining environmental histories of fish. Canadian Journal of Fisheries and Aquatic Sciences 59:1796–1808.

Elsdon, T. S., B. K. Wells, S. E. Campana, B. M. Gillanders, C. M. Jones, K. E. Limburg, D. H. Secor, S. R. Thorrold, and B. D. Walther. 2008. Otolith chemistry to describe movements and life-history parameters of fishes: hypotheses, assumptions, limitations and inferences. Oceanography and Marine Biology 46:297–330.

Fabrizio, M. C., J. P. Manderson, and J. P. Pessutti. 2013. Habitat associations and dispersal of black sea bass from a mid-Atlantic Bight reef. Marine Ecology Progress Series 482:241–253.

Fabrizio, M. C., J. P. Manderson, and J. P. Pessutti. 2014. Home range and seasonal movements

of black sea bass (Centropristis striata) during their inshore residency at a reef in the mid-Atlantic Bight. Fishery Bulletin 112:82–97.

Farrell, J., and S. E. Campana. 1996. Regulation of calcium and strontium deposition on the otoliths of juvenile tilapia, Oreochromis niloticus. Comparative Biochemistry and Physiology 115A(2):103–109.

Fogarty, M., L. Incze, R. Wahle, D. Mountain, A. Robinson, A. Pershing, K. Hayhoe, A. Richards, and J. Manning. 2007. Potential climate change impacts on marine resources of the northeastern United States. Climate Change and Marine Resources Impacts:1–33.

Fowler, A. J., S. E. Campana, C. M. Jones, and S. R. Thorrold. 1995a. Experimental assessment of the effect of temperature and salinity on elemental composition of otoliths using laser ablation ICPMS. Canadian Journal of Fisheries and Aquatic Sciences 52:1431–1441.

Fowler, A. J., S. E. Campana, C. M. Jones, and S. R. Thorrold. 1995b. Experimental assessment of the effect of temperature and salinity on elemental composition of otoliths using solution-based ICPMS. Canadian Journal of Fisheries & Aquatic Sciences 52:1421–1430.

Fox, J., and S. Weisberg. 2019. An {R} Companion to Applied Regression.

Gillanders, B. M. 2002. Connectivity between juvenile and adult fish populations: Do adults remain near their recruitment estuaries? Marine Ecology Progress Series 240:215–223.

Hamer, P. A., and G. P. Jenkins. 2007. Comparison of spatial variation in otolith chemistry of two fish species and relationships with water chemistry and otolith growth. Journal of Fish Biology 71:1035–1055.

Hartig, F. 2021. DHARMa: Residual diagnostics for hierarchical (Multi-Level/Mixed) Regression Models.

Hoff, G. R., and L. A. Fuiman. 1995. Environmentally induced variation in elemental

composition of red drum (Sciaenops ocellatus) otoliths. Bulletin of Marine Science 56(2):578–591.

Hothorn, T., F. Bretz, and P. Westfall. 2008. Simultaneous inference in general parametric models. Biometrical Journal 50(3):346–363.

Van Hulten, M., R. Middag, J.-C. Dutay, H. De Baar, M. Roy-Barman, M. Gehlen, A. Tagliabue, and A. Sterl. 2017. Manganese in the west Atlantic Ocean in the context of the first global ocean circulation model of manganese. Biogeosciences 14:1123–1152.

Hüssy, K., K. E. Limburg, H. de Pontual, O. R. B. Thomas, P. K. Cook, Y. Heimbrand, M. Blass, and A. M. Sturrock. 2020. Trace Element Patterns in Otoliths: The Role of Biomineralization. Reviews in Fisheries Science and Aquaculture:1–33. Taylor & Francis.

Javor, B., and E. Dorval. 2014. Geography and ontogeny influence the stable oxygen and carbon isotopes of otoliths of Pacific sardine in the California Current. Fisheries Research 154:1–10.

Kalish, J. M. 1989. Otolith microchemistry: validation of the effects of physiology, age and environment on otolith composition. Journal of Experimental Marine Biology and Ecology 132:151–178.

Kalish, J. M. 1991. 13C and 18O isotopic disequilibria in fish otoliths: metabolic and kinetic effects. Marine Ecology Progress Series 75:191–203.

Kerr, L. A., and S. E. Campana. 2014. Chemical composition of fish hard parts as a natural marker of fish stocks. Pages 205–234 *in* S. X. Cadrin, K. D. Friedland, and J. R. Waldman, editors. Stock Identification Methods: Applications in Fishery Science, 2nd edition. Academic Press, New York, USA.

Kerr, L. A., D. H. Secor, and R. T. Kraus. 2007. Stable isotope (δ13C and δ18O) and Sr/Ca

composition of otoliths as proxies for environmental salinity experienced by an estuarine fish. Marine Ecology Progress Series 349:245–253.

Kerr, L. A., Z. T. Whitener, S. X. Cadrin, M. R. Morse, D. H. Secor, and W. Golet. 2020. Mixed stock origin of Atlantic bluefin tuna in the U.S. rod and reel fishery (Gulf of Maine) and implications for fisheries management. Fisheries Research 224:1–11.

Kleisner, K. M., M. J. Fogarty, S. McGee, A. Barnett, P. Fratantoni, J. Greene, J. A. Hare, S. M. Lucey, C. McGuire, J. Odell, V. S. Saba, L. Smith, K. J. Weaver, and M. L. Pinsky. 2016. The effects of sub-regional climate velocity on the distribution and spatial extent of marine species assemblages. PLoS ONE 11(2):1–21.

Kleisner, K. M., M. J. Fogarty, S. McGee, J. A. Hare, S. Moret, C. T. Perretti, and V. S. Saba. 2017. Marine species distribution shifts on the U.S. Northeast Continental Shelf under continued ocean warming. Progress in Oceanography 153:24–36.

Kolek, D. 1990. Homing of black sea bass, Centropristis striata, in Nantucket Sound, with comments on seasonal distribution, growth rates, and fisheries of the species. MADMF Black Sea Bass Investigations Internal Report:2–9.

Koob, E. R., S. P. Elzey, J. W. Mandelman, and M. P. Armstrong. 2021. Age validation of the northern stock of black sea bass (Centropristis striata) in the Atlantic Ocean. Fishery Bulletin 119:261–273.

Kremling, K. 1985. The distribution of cadmium, copper, nickel, manganese, and aluminium in surface waters of the open Atlantic and European shelf area. Deep Sea Research 32(5):531–555.

Laugier, F., E. Feunteun, C. Pecheyran, and A. Carpentier. 2015. Life history of the small sandeel, Ammodytes tobianus, inferred from otolith microchemistry. A methodological

approach. Estuarine, Coastal and Shelf Science 165:237–246.

Lenth, R. 2019. Emmeans: estimated marginal means, aka least-squares means. R package version 1.4.3.01.

Liaw, A., and M. Wiener. 2002. Classification and regression by randomForest. R News 2(3):18–22.

Loewen, T. N., J. D. Reist, P. Yang, A. Koleszar, J. A. Babaluk, N. Mochnacz, and N. M. Halden. 2015. Discrimination of northern form dolly varden char (Salvelinus malma malma) stocks of the North Slope, Yukon and Northwest Territories, Canada via otolith trace elements and 87Sr/86Sr isotopes. Fisheries Research 170:116–124.

Maguffee, A. C., R. Reilly, R. Clark, and M. L. Jones. 2019. Examining the potential of otolith chemistry to determine natal origins of wild Lake Michigan Chinook Salmon. Canadian Journal of Fisheries and Aquatic Sciences 76:2035–2044.

Manel, S., O. Gaggiotti, and R. Waples. 2005. Assignment methods: matching biological questions with appropriate techniques. Trends in Ecology and Evolution 20(3):136–142.

McBride, R. S. 2017. Supplemental material to: Black sea bass, Centropristis striata, reproduction and first-year growth in New England: northward expansion of spawning and nursery grounds in a warming Gulf of Maine. Fishery Bulletin 116:1–7.

McBride, R. S., M. K. Tweedie, and K. Oliveira. 2018. Reproduction, first-year growth, and expansion of spawning and nursery grounds of black sea bass (Centropristis striata) into a warming Gulf of Maine. Fishery Bulletin 116:323–336.

McMahan, M. D. 2017. Ecological and socioeconomic implications of a northern range expansion of black sea bass, Centropristis striata. Doctoral dissertation. Northeastern University, Boston, Massachusetts.

McMahan, M. D., G. D. Sherwood, and J. H. Grabowski. 2020. Geographic variation in life-history traits of black sea bass (Centropristis striata) during a rapid range expansion. Frontiers in Marine Science 7(567758):1–15.

Mercer, L. P. 1978. The reproductive biology and population dynamics of black sea bass, Centropristis striata. Doctoral dissertation. The College of William and Mary, Williamsburg, Virginia.

Miller, A. S., G. R. Shepherd, and P. S. Fratantoni. 2016. Offshore habitat preference of overwintering juvenile and adult black sea bass, Centropristis striata, and the relationship to year-class success. PLoS ONE 11(1):1–19.

Moser, J., and G. R. Shepherd. 2009. Seasonal distribution and movement of black sea bass (Centropristis striata) in the northwest Atlantic as determined from a mark-recapture experiment. Journal of Northwest Atlantic Fishery Science 40:17–28. Northwest Atlantic Fisheries Organization.

Musick, J. A., and L. P. Mercer. 1977. Seasonal distribution of black sea bass, Centropristis striata, in the Mid-Atlantic Bight with comments on the ecology and fisheries of the species. Transactions of the American Fisheries Society 106(1):12–25.

NEFSC. 2017. 62nd Northeast regional stock assessment workshop. Northeast Fisheries Science Center Reference Assessment Summary Report:1–36.

Nye, J. A., J. S. Link, J. A. Hare, and W. J. Overholtz. 2009. Changing spatial distribution of fish stocks in relation to climate and population size on the Northeast United States continental shelf. Marine Ecology Progress Series 393:111–129.

Office of Coast Survey. 2022. NOAA Raster Navigational Charts (RNC). https://www.fisheries.noaa.gov/inport/item/39966.

Pershing, A. J., M. A. Alexander, C. M. Hernandez, L. A. Kerr, A. Le Bris, K. E. Mills, J. A. Nye, N. R. Record, H. A. Scannell, J. D. Scott, G. D. Sherwood, and A. C. Thomas. 2015. Slow adaptation in the face of rapid warming leads to collapse of the Gulf of Maine cod fishery. Science 350(6262):809–812.

R Core Team. 2019. R: a language and environment for statistical computing. R Foundation for Statistical Computing. Vienna, Austria.

Ranaldi, M. M., and M. M. Gagnon. 2008. Zinc incorporation in the otoliths of juvenile pink snapper (Pagrus auratus Forster): The influence of dietary versus waterborne sources. Journal of Experimental Marine Biology and Ecology 360:56–62.

Ruttenberg, B. I., S. L. Hamilton, M. J. H. Hickford, G. L. Paradis, M. S. Sheehy, J. D. Standish, O. Ben-Tzvi, and R. R. Warner. 2005. Elevated levels of trace elements in cores of otoliths and their potential for use as natural tags. Marine Ecology Progress Series 297:273–281.

Sadovy, Y., and K. P. Severin. 1992. Trace elements in biogenic aragonite: correlation of body growth rate and strontium levels in the otoliths of the white grunt, Haemulon Plumieri (Pisces: Haemulidae). Bulletin of Marine Science 50(2):237–257.

Sadovy, Y., and K. P. Severin. 1994. Elemental patterns in red hind (Epinephelus guftatus) otoliths from Bermuda and Puerto Rico reflect growth rate, not temperature. Canadian Journal of Fisheries and Aquatic Sciences 51:133–141.

SARC. 2016. Proposed partitioning of northern black sea bass stock for purposes of developing spatial stock assessment models. Black Sea Bass Benchmark Stock Assessment Review Term of Reference - Spatial Issues:1–40.

Secor, D. H. 1999. Specifying divergent migrations in the concept of stock: the contingent hypothesis. Fisheries Research 43:13–34.

Shiller, A. M. 1997. Manganese in surface waters of the Atlantic Ocean. Geophysical Research Letters 24(12):1495–1498.

Slesinger, E., O. P. Jensen, and G. Saba. 2021. Spawning phenology of a rapidly shifting marine fish species throughout its range. ICES Journal of Marine Science (January).

Steer, M. A., A. J. Fowler, and B. M. Gillanders. 2009. Age-related movement patterns and population structuring in southern garfish, Hyporhamphus melanochir, inferred from otolith chemistry. Fisheries Management and Ecology 16:265–278.

Sturrock, A. M., E. Hunter, J. A. Milton, R. C. Johnson, C. P. Waring, and C. N. Trueman. 2015. Quantifying physiological influences on otolith microchemistry. Methods in Ecology and Evolution 6:806–816.

Tanner, S. E., P. Reis-Santos, and H. N. Cabral. 2016. Otolith chemistry in stock delineation: a brief overview, current challenges and future prospects. Fisheries Research 173:206–213.

Tanner, S. E., P. Reis-Santos, R. P. Vasconcelos, S. França, S. R. Thorrold, and H. N. Cabral. 2012. Otolith geochemistry discriminates among estuarine nursery areas of Solea solea and S. senegalensis over time. Marine Ecology Progress Series 452:193–203.

Thorrold, S. R., S. E. Campana, C. M. Jones, and P. K. Swart. 1997a. Factors determining δ 13C and δ 18O fractionation in aragonitic otoliths of marine fish. Geochimica et Cosmochimica Acta 61(14):2909–2919.

Thorrold, S. R., C. M. Jones, and S. E. Campana. 1997b. Response of otolith microchemistry to environmental variations experienced by larval and juvenile Atlantic croaker (Micropogonias undulatus). Limnology and Oceanography 42(1):102–111.

Thorrold, S. R., C. M. Jones, P. K. Swart, and T. E. Targett. 1998. Accurate classification of juvenile weakfish Cynoscion regalis to estuarine nursery areas based on chemical signatures

in otoliths. Marine Ecology Progress Series 173:253–265.

Thresher, R. E. 1999. Elemental composition of otoliths as a stock delineator in fishes. Fisheries Research 43:165–204.

Tournois, J., F. Ferraton, L. Velez, D. J. McKenzie, C. Aliaume, L. Mercier, and A. M. Darnaude. 2013. Temporal stability of otolith elemental fingerprints discriminates among lagoon nursery habitats. Estuarine, Coastal and Shelf Science 131:182–193.

Townsend, D. W., R. L. Radtke, D. P. Malone, and J. P. Wallinga. 1995. Use of otolith strontium:calcium ratios for hindcasting larval cod Gadus morhua distributions relative to water masses on Georges Bank. Marine Ecology Progress Series 119:37–44.

U.S. IOOS. 2023. U.S. Integrated Ocean Observing System. [online database]. Silver Spring, MD. Available: https://ioos.noaa.gov/data/access-ioos-data/

Venables, W. N., and B. D. Ripley. 2002. Modern applied statistics, 4th edition. Springer, New York.

Wenner, C. A., W. A. Roumillat, and C. W. Waltz. 1986. Contributions to the life history of black sea bass, Centropristis striata, off the Southeastern United States. Fishery Bulletin 84(3):723–741.

Wickham, H. 2016. ggplot2: elegant graphics for data analysis. Springer-Verlag, New York.

Wuenschel, M. J., R. S. McBride, and G. R. Fitzhugh. 2013. Relations between total gonad energy and physiological measures of condition in the period leading up to spawning: results of a laboratory experiment on black sea bass (Centropristis striata). Fisheries Research 138:110–119.

Tables

TABLE 1. Sample data for Black Sea Bass used in microchemical analyses by collection region: ME (Maine), SNE (Southern New England), and MAB (mid-Atlantic Bight). Footnotes indicate institutions that originally collected the samples as well as how and when they were collected.

Region	*n*	Months collected	Length (cm)		Age range (years)	Year classes	Sex composition (*n*)			Gear type
			Mean	S.E.			Female	Male	Unk	
ME [a] mixed stock	46	Jun-Nov	26.7	0.8	2-4	2010-2014	29	16	1	hook & line; trap
SNE [a, b, c] spawning adults	43	May-Aug	36.3	0.9	2-6	2010-2015	22	21	0	trap; trawl
MAB [d, e] spawning adults	44	Jul-Sep	29.4	0.8	2-6	2010-2015	17	27	0	trap; trawl

[a] Northeastern University. Samples collected from commercial and recreational lobster traps, Ventless Survey traps, and hook and line from June through November in 2013-2016.

[b] Massachusetts Division of Marine Fisheries. Samples collected from Ventless Survey traps and the Resource Assessment Bottom Trawl Survey from May through November in 2013-2017.

[c] Commercial Fisheries Research Foundation, in collaboration with Rhode Island Department of Environmental Management (RI-DEM) and Virginia Institute of Marine Science. Samples collected from the commercial otter trawl and fish pot fisheries in June and July of 2017.

[d] Northeast Fisheries Science Center (NEFSC). Samples collected from the NEFSC Bottom Trawl Survey in April and September in 2015-2017.

[e] Rutgers University. Samples collected from Ventless Survey Traps in July and August in 2017.

TABLE 2. Black Sea Bass core otolith isotopic and elemental ratio untransformed mean signatures ± standard error for each region ME (Maine), SNE (Southern New England), and MAB (mid-Atlantic Bight). Wald X^2 (df = 2; alpha = 0.05) values and significance (*P*) results for each variable are also provided. Samples were randomly selected from archived black sea bass otoliths originally collected by collaborative institutions from May through November in 2013-2017.

	δ18O (VPDB ‰)	δ13C (VPDB ‰)	Mg:Ca (ppm)	Mn:Ca (ppm)	Cu:Ca (ppm)	Zn:Ca (ppm)	Sr:Ca (ppm)	Ba:Ca (ppm)
ME	-1.47 ± 0.06	-3.74 ± 0.12	43.0 ± 2.44	6.66 ± 0.79	1.78 ± 0.26	1.29 ± 0.09	1729 ± 22.7	9.55 ± 0.91
SNE	-1.60 ± 0.07	-3.72 ± 0.10	37.4 ± 1.99	8.01 ± 1.18	3.45 ± 0.73	1.68 ± 0.14	1718 ± 23.7	9.00 ± 0.79
MAB	-1.10 ± 0.09	-3.93 ±0.09	28.6 ± 1.02	10.2 ± 0.82	5.22 ± 1.28	1.39 ± 0.15	1684 ± 22.9	4.32 ± 0.45
X^2	20.2	2.68	37.9	10.6	26.8	6.99	0.80	26.5
P	< 0.0001	0.262	< 0.0001	< 0.010	< 0.0001	0.030	0.671	< 0.0001

Figures

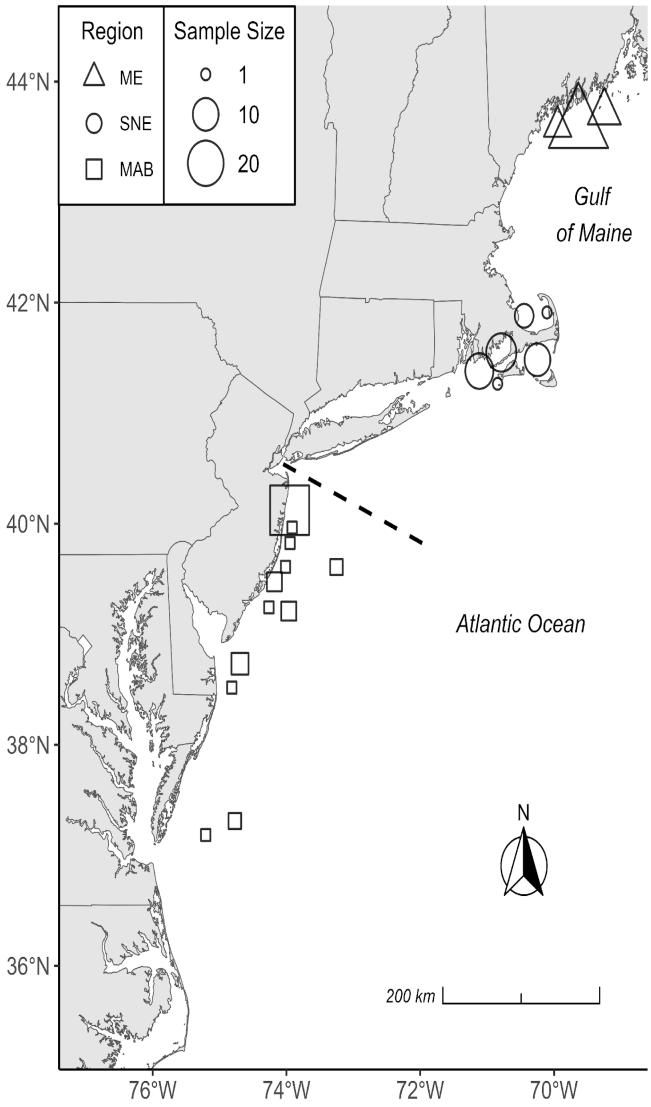

FIGURE 1. Map of Black Sea Bass sample capture locations along the northeast United States coast as grouped in this study: Maine (ME), Southern New England (SNE), and mid-Atlantic Bight (MAB). Samples were randomly selected from archived black sea bass otoliths originally collected by collaborative institutions from May through November in 2013-2017. Symbol size

is weighted by sample size at each location. Dashed line indicates the Black Sea Bass population separation at the Hudson Canyon.

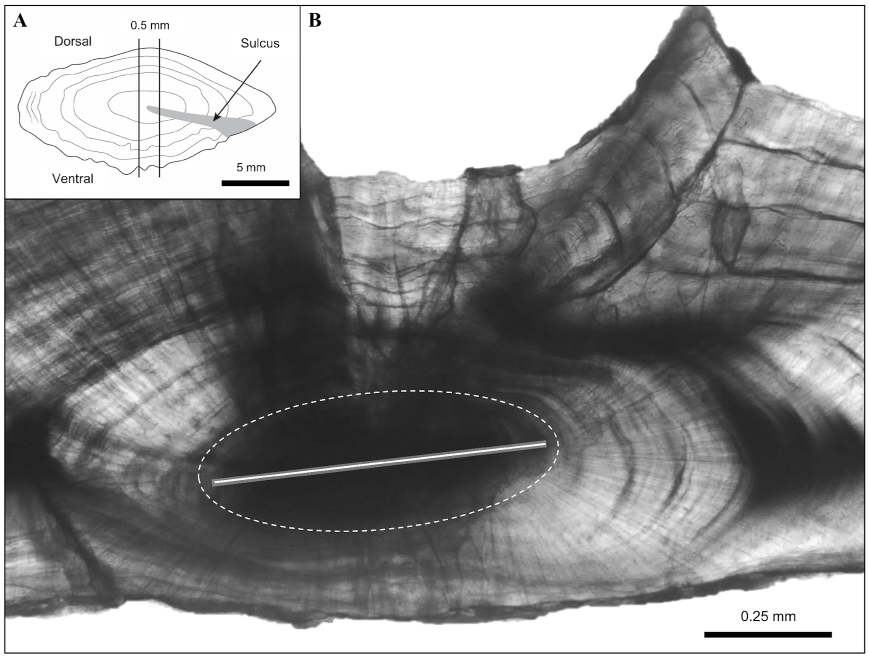

FIGURE 2. (A) Positioning of the section (0.5-mm thick) taken through the core of a whole Black Sea Bass otolith. (B) Area of microchemical sampling on a sectioned Black Sea Bass otolith. The thick gray band represents the pre-ablation transect for trace element analysis (LA-ICPMS) while the thinner white line within shows the sampling transect. Milled otolith material used in stable isotope analysis (GB-IRMS) is shown as the area within the dotted white line (i.e., the opaque region of the core).

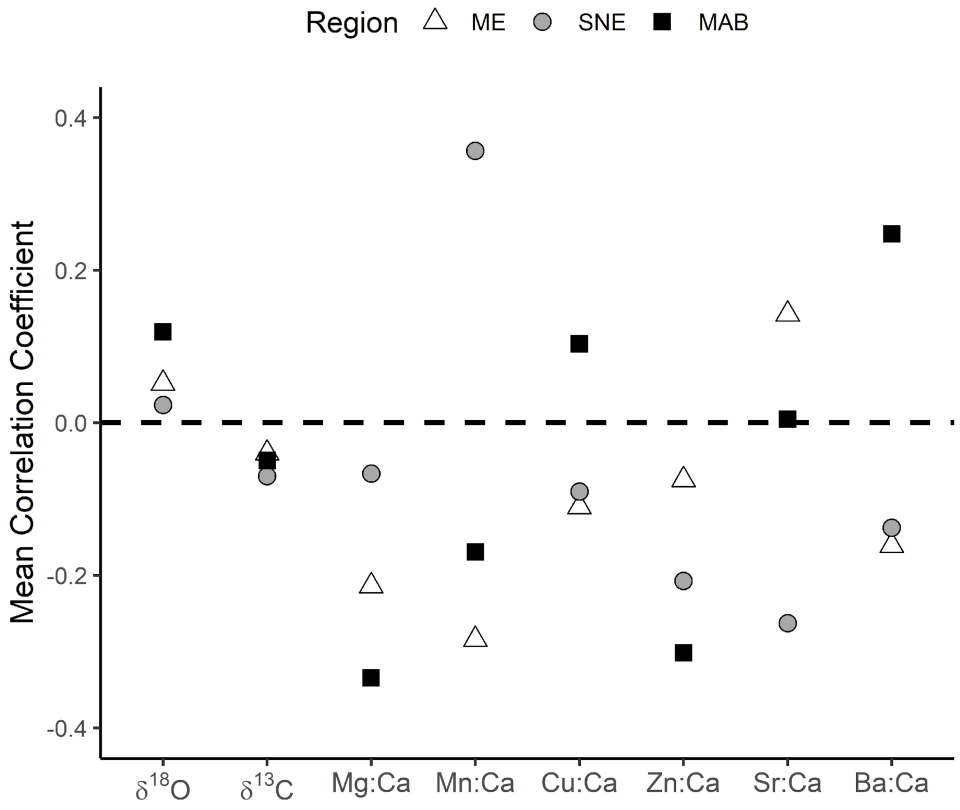

FIGURE 3. Mean Pearson's correlation coefficients between core measurements and isotopic and elemental ratios for each region: Maine (ME), Southern New England (SNE), and the mid-Atlantic Bight (MAB).

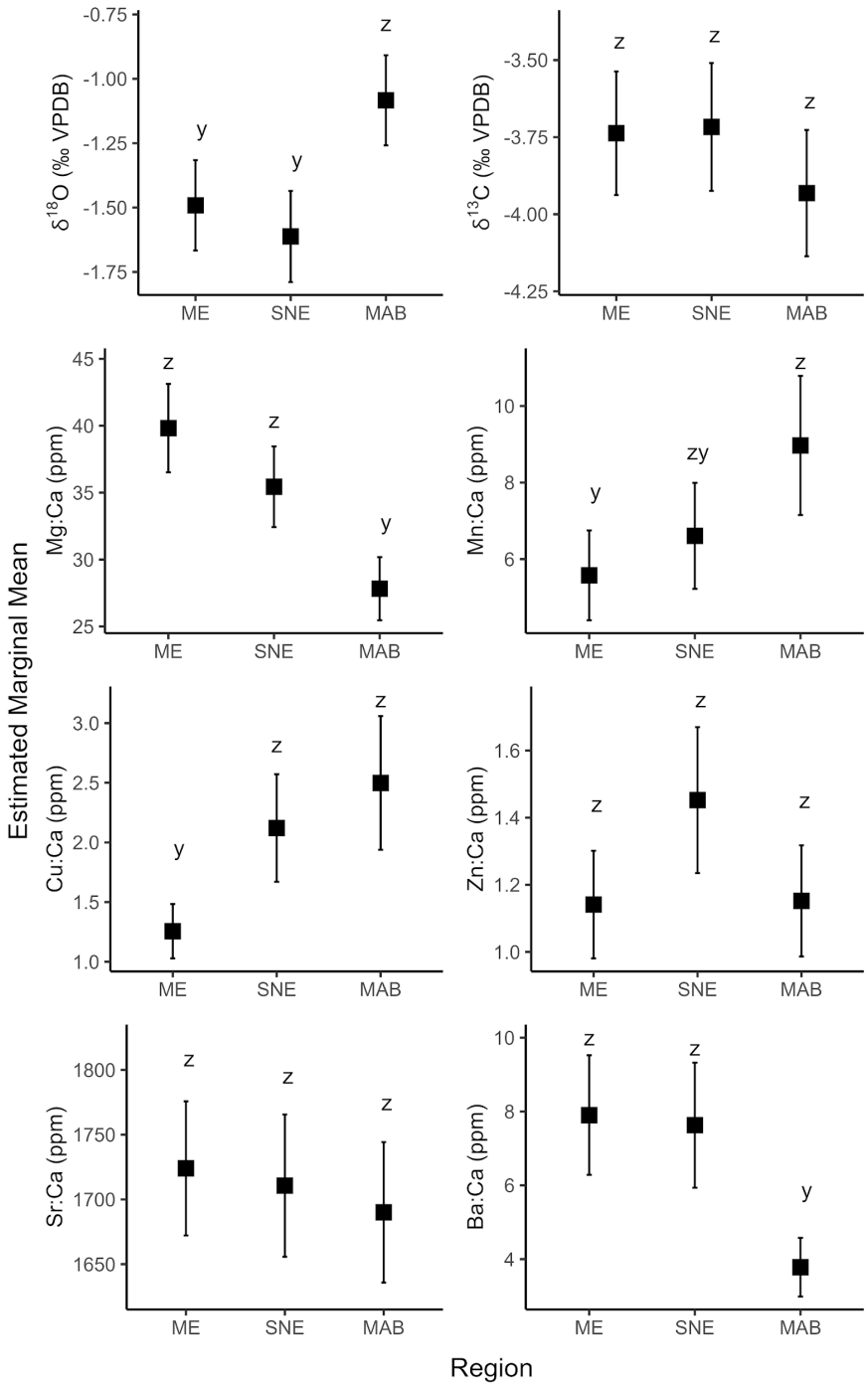

FIGURE 4. Estimated marginal means of each isotopic and elemental ratio by region from results of the linear mixed models. Letters denote significant differences (Wald X^2, alpha = 0.05). Error bars represent two standard errors of the estimated marginal mean.

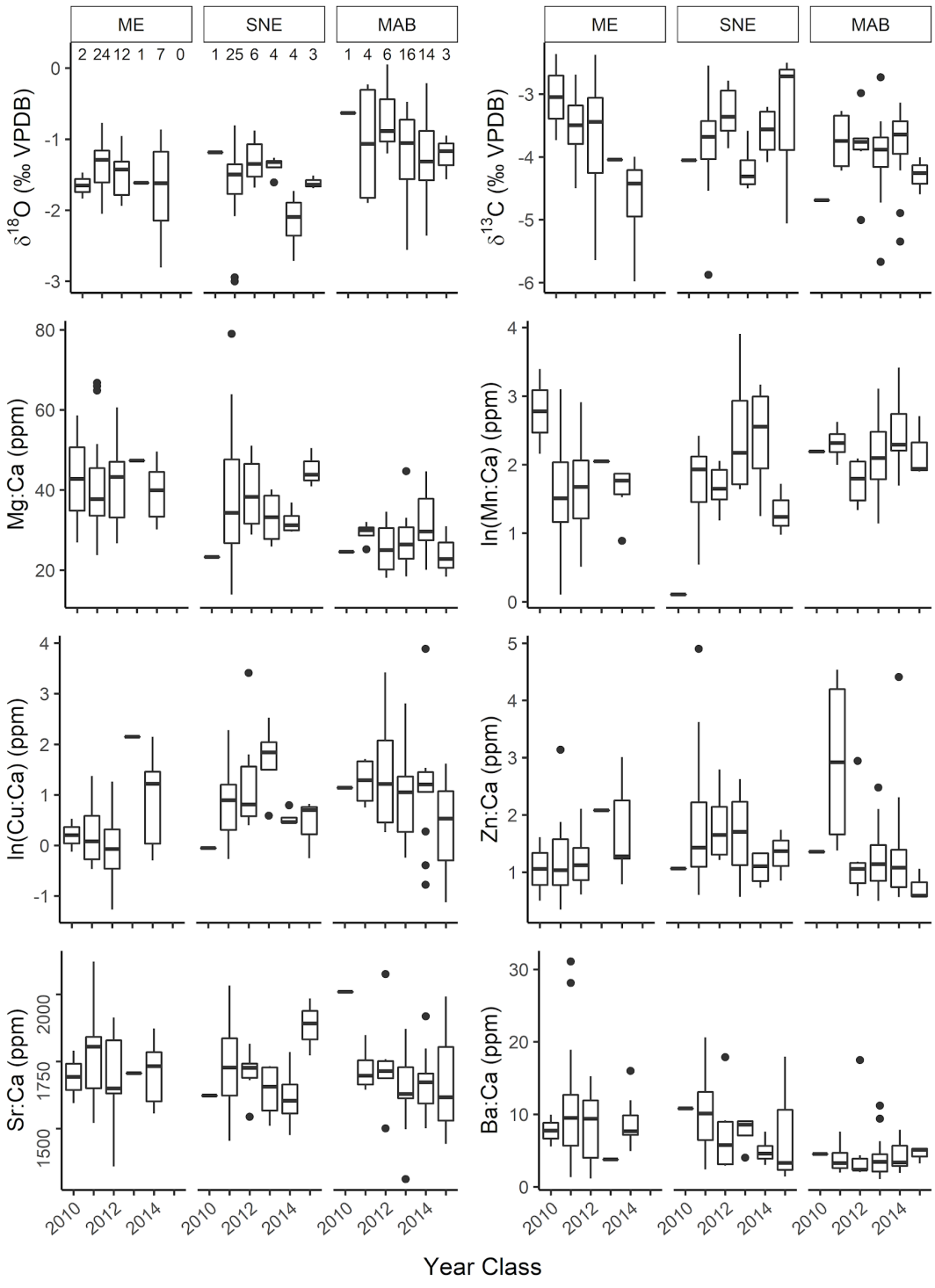

FIGURE A.1. Boxplots for each isotopic and elemental ratio by year class and region. Boxplots represent median (thick horizontal line), the 25-75 percentile (boxed area above and below

median), the 95% confidence limits (thin vertical lines), and outliers (points). Regions are as follows: Maine (ME), Southern New England (SNE), and the mid-Atlantic Bight (MAB). Numbers on the first plot indicate sample sizes and apply to all other plots; note the small sample sizes in some year class and region combinations.

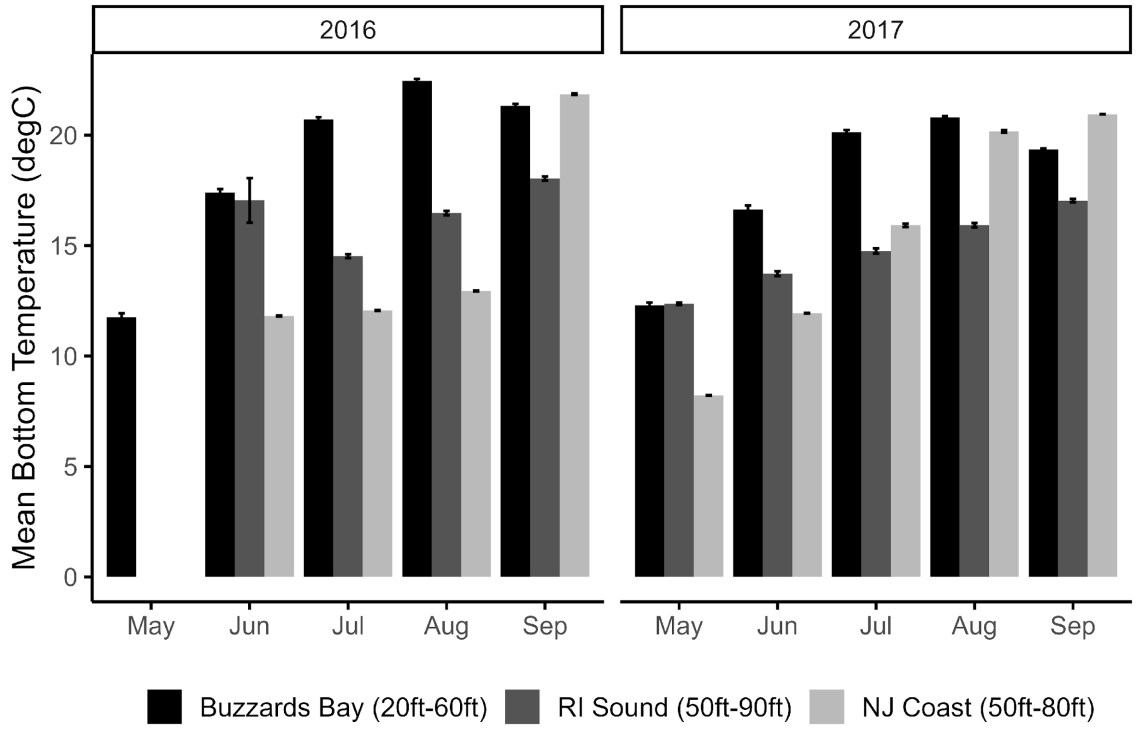

FIGURE A.2. Bar chart of mean bottom temperatures (^{0}C) for Buzzards Bay, Rhode Island (RI) Sound, and New Jersey (NJ) coast from 2016-2017. Buzzards Bay temperature data was collected from Massachusetts Division of Marine Fisheries (MADMF) bottom temperature loggers and the Ventless Trap Survey. RI Sound temperature data also came from MADMF Ventless Trap Survey. NJ coast data was collected from the NJ Ventless Trap Survey and the U.S. Integrated Ocean Observing System underwater gliders (U.S. IOOS 2023). Data from the U.S.

IOOS was bound by sampling locations and depths at which most of the Black Sea Bass in this study were collected in this region (between 38.2 N and 40.2 N, and between -75.2 W and -73.89 W; 50-80ft deep). Error bars are two standard errors of the mean.